https://doi.org/10.5194/acp-2022-327
Preprint. Discussion started: 24 May 2022

Atmospheric Chemistry and Physics Discussions

Modeling Diurnal Variation of SOA Formation via Multiphase Reactions of Biogenic Hydrocarbons

Sanghee Han[1], Myoseon Jang[1]

[1]Department of Environmental Engineering Science, University of Florida, Gainesville, Florida, USA

Correspondence to: Myoseon Jang (mjang@ufl.edu)

Abstract.

The daytime oxidation of biogenic hydrocarbons is attributed to both OH radicals and O_3, while nighttime chemistry is dominated by the reaction with O_3 and NO_3 radicals. Here, the diurnal pattern of Secondary Organic Aerosol (SOA) originating from biogenic hydrocarbons was intensively evaluated under varying environmental conditions (temperature, humidity, sunlight intensity, NO_x levels, and seed conditions) by using the UNIfied Partitioning Aerosol phase Reaction (UNIPAR) model, which comprises multiphase gas-particle partitioning and in-particle chemistry. The oxidized products of three different hydrocarbons (isoprene, α-pinene, and β-caryophyllene) were predicted by using near explicit gas mechanisms for four different oxidation paths (OH, O_3, NO_3, and $O(^3P)$) during day and night. The gas mechanisms implemented the Master Chemical Mechanism (MCM v3.3.1), the reactions that formed low volatility products via peroxy radical (RO_2) autoxidation, and self- and cross-reactions of nitrate-origin RO_2. In the model, oxygenated products were then classified into volatility-reactivity base lumping species, which were dynamically constructed under varying NO_x levels and aging scales. To increase feasibility, the UNIPAR model that equipped mathematical equations for stoichiometric coefficients and physicochemical parameters of lumping species was integrated with the SAPRC gas mechanism. The predictability of the UNIPAR model was demonstrated by simulating chamber-generated SOA data under varying environments day and night. Overall, the SOA simulation decoupled to each oxidation path indicated that the nighttime isoprene SOA formation was dominated by the NO_3-driven oxidation, regardless of NO_x levels. However, the oxidation path to produce the nighttime α-pinene SOA gradually transited from the NO_3-initiated reaction to ozonolysis as NO_x levels decreased. For daytime SOA formation, both isoprene and α-pinene were dominated by the OH-radical initiated oxidation. The contribution of the $O(^3P)$ path to all biogenic SOA formation was negligible in daytime. Sunlight during daytime promotes the decomposition of oxidized products via photolysis and thus, reduces SOA yields. Nighttime α-pinene SOA yields were significantly higher than daytime SOA yields, although the nighttime α-pinene SOA yields gradually decreased with decreasing NO_x levels. For isoprene, nighttime chemistry yielded higher SOA mass than daytime at the higher NO_x level (isoprene/NO_x > 5 ppbC/ppb). The daytime isoprene oxidation at the low NO_x level formed epoxy-diols that significantly contributed SOA formation via heterogeneous chemistry. For isoprene and α-pinene, daytime SOA yields gradually increased with decreasing NO_x levels. The daytime SOA produced more highly oxidized multifunctional products and thus, it was generally more sensitive to the aqueous reactions than the nighttime SOA. β-Caryophyllene, which rapidly oxidized and produced SOA with high yields, showed a relatively small variation in SOA yields from changes in environmental conditions (i.e., NO_x levels, seed conditions, and diurnal pattern), and its SOA formation was mainly attributed to ozonolysis day and night. To mimic the nighttime α-pinene SOA formation under the polluted urban atmosphere, α-pinene SOA formation was simulated in the presence of gasoline fuel. The simulation suggested the growth of α-pinene SOA in the presence of gasoline fuel gas by the enhancement of the ozonolysis path under the excess amount of ozone, which is typical in urban air. We concluded that the oxidation of the biogenic hydrocarbon with O_3 or NO_3 radicals is a source to produce a sizable amount of nocturnal SOA, despite of the low emission at night.

https://doi.org/10.5194/acp-2022-327
Preprint. Discussion started: 24 May 2022

Atmospheric Chemistry and Physics Discussions

1 Introduction

Organic aerosol in the ambient air has been a well-known factor to impact human health (Pye et al., 2022;Mauderly and Chow, 2008) and climate change (Tsigaridis and Kanakidou, 2018;Kanakidou et al., 2005). A large portion of organic aerosol is secondary organic aerosol (SOA) produced from the oxidation process of hydrocarbons (HCs), emitted from both biogenic and anthropogenic sources (Hallquist et al., 2009;Jimenez et al., 2009). In particular, the global emission of biogenic HCs, which is more than two-thirds of the total HC emissions, dominate over that of anthropogenic HCs by an order magnitude (Guenther et al., 1995;Goldstein and Galbally, 2007;Sindelarova et al., 2014). These biogenic HCs contain olefinic (C=C) bonds that are highly reactive towards various oxidants (i.e., OH radicals, NO_3 radicals, and O_3) (Atkinson and Arey, 2003). Furthermore, the SOA from the oxidation of biogenic HCs is considerable in a global budget of SOA. For example, the annual global SOA production rates from monoterpene and isoprene is more than 50% of the global SOA formation, 19.9 and 19.6 Tg (SOA) a^{-1}, respectively (Kelly et al., 2018).

In the daytime, a large amount of biogenic HC is oxidized mainly with OH radicals and O_3 to form a considerable SOA burden (Zhang et al., 2018;Carlton et al., 2009;Sakulyanontvittaya et al., 2008;Barreira et al., 2021). The photooxidation of NO_x enhances the production of O_3 and regenerate OH radicals, increasing the consumption of biogenic HCs and SOA formation. In nighttime, however, the oxidation of biogenic HCs with the OH radical is minimized, while that of biogenic HCs is processed dominantly by O_3 and NO_3 radicals. The O_3 that is generated in daytime is persistent at nighttime. A NO_3 radical that forms via the reaction of O_3 with NO_2 can also be sustainable in nighttime. Thus, the oxidation pathways of biogenic HCs can change diurnally with different NO_x levels, humidity, and temperature, and ultimately influence SOA formation. For example, the oxidation of isoprene with the NO_3 radical can rapidly produce nitrate containing products, such as C_5-nitroxycarbonyl and C_5-hydroxynitrate, up to 80% of gas products from the isoprene-NO_3 oxidation (Kwok et al., 1996;Barnes et al., 1990). Numerous studies recently have also shown the important role of the NO_3 radical on the production of SOA, suggesting the emission of NO_x from human activities increases the biogenic SOA mass (Ng et al., 2008;Bonn and Moorgat, 2002;Jaoui et al., 2013;Rollins et al., 2012). Furthermore, the variation of the inorganic seed effects on SOA formation can be significant by different oxidation pathways, which produce different product distributions.

In current air quality models, the partitioning-based SOA models semi-empirically established a relationship between the absorbing organic matter (OM) concentration and the SOA yields by using a simple model parameters for two (Odum et al., 1996) or more surrogate products (Donahue et al., 2006). The oxidation of biogenic HCs was approached by the reaction with four major oxidants: OH radicals, NO_3 radicals, O_3, and $O(^3P)$. Consequently, the biogenic SOA formation is predicted with the surrogate products originating from these four major oxidations. However, the gas phase reactions were not additive due to the various cross reactions. For example, the 1st generation of oxidation products initiated by the ozone mechanism can react with the OH radical. The product distribution originating from a specific oxidant can also influenced by the NO_x level and atmospheric gas aging.

Numerous studies have shown the importance of the aerosol phase reaction, yielding the non-volatile species or oligomeric matter, of reactive organic species (i.e., aldehydes and epoxides) in aerosol phase (Jang et al., 2002;Woo et al., 2013;Altieri et al., 2006;Ervens et al., 2004;Liggio et al., 2005). The typical partitioning-based models include organic-phase oligomerization of organic species, but they do not fully treat the SOA formation via the aqueous reactions in the presence of inorganic salted aqueous phase. To predict SOA formation via the multiphase reaction of HCs, the UNIfied Partitioning Aerosol-phase Reaction (UNIPAR) model has been developed (Beardsley and Jang, 2016;Im et al., 2014;Zhou et al., 2019). UNIPAR streamlines the gas oxidation integrated with explicit mechanisms, multiphase partitioning, and aerosol-phase reactions in both organic and inorganic phases. This model has been demonstrated by the SOA produced from various aromatic HCs (Im et al., 2014;Zhou et al., 2019;Han and Jang, 2022), monoterpenes (Yu et al., 2021), and isoprene (Beardsley and Jang, 2016).

https://doi.org/10.5194/acp-2022-327
Preprint. Discussion started: 24 May 2022


Atmospheric Chemistry and Physics Discussions

In this study, to predict the diurnal pattern of biogenic SOA formation, the UNIPAR model was extended to biogenic SOA formation at nighttime. Lumping species and their stoichiometric coefficient and physicochemical parameters from the explicit gas mechanisms were individually generated from the four different oxidation pathways with OH radicals, O_3, NO_3 radicals, and $O(^3P)$. To improve the feasibility, the UNIPAR model was integrated with the SAPRC07TC gas mechanism (UNIPAR-SAPRC), providing the HC consumption by each oxidant. The resulting model allows the prediction of biogenic SOA in day and night with the dynamically controlled product distribution by oxidation of gas simulation. The potential SOA yield of biogenic HCs via four different oxidation paths were investigated by simulation of the UNIPAR-SAPRC model and applied to clarify the diurnal patterns in biogenic SOA formation under varying NO_x levels, temperature, and seed conditions. Additionally, the UNIPAR-SAPRC model was utilized to analyze the impact of anthropogenic emissions on biogenic SOA formations.

2 Chamber experiment

The chamber experiments to produce SOA from the oxidation process of biogenic HCs were conducted in the University of Florida Atmospheric PHotochemical Outdoor Reactor (UF-APHOR) chamber located on the rooftop of Black Hall (29.64°, -82.34°) at the University of Florida, Gainesville, Florida. The detailed configuration of the UF-APHOR and the experimental procedures were previously reported (Beardsley and Jang, 2016;Im et al., 2014;Zhou et al., 2019). In brief, UF-APHOR chamber is a dual chamber (52 m^3 (East) + 52 m^3 (West)) made with Fluorinated Ethylene Propylene (FEP) Teflon film. For daytime experiments, the injection was done before sunrise, and the experiments started at sunrise, conducted for 10 to 12 hours. The NO_x levels were controlled by NO injected from the 2% NO cylinder under the air flow and classified into high NO_x (HC/NO_x < 5.5 ppbC/ppb) and low NO_x level (HC/NO_x > 5.5 ppbC/ppb) based on the initial concentration of HC and NO. Inorganic seed aerosols (sulfuric acid, (SA), wet ammonium sulfate, (wet-AS), and dry ammonium sulfate (dry-AS)) were injected into the chamber to evaluate the effects of wet inorganic seed on SOA formation. For nighttime experiments, the injection and experiments began after sunset to avoid photochemical reaction, and experiments were conducted for 3 to 5 hours. O_3 was injected first into the chamber by using the O_3 generator, and NO_x condition was controlled by NO_2. NO_2 was injected from the 2% NO_2 cylinder into the chamber under the air flow. Nighttime biogenic SOA formation was observed under the three different NO_x levels (i.e., O_3 only, low NO_x (HC/NO_x > 5.5 ppbC/ppb) and high NO_x level (HC/NO_x < 5.5 ppbC/ppb)). Three different biogenic HCs (isoprene (C_5H_8, 99%, Aldrich), α-pinene ($C_{10}H_{16}$, 98% Aldrich), and β-caryophyllene ($C_{15}H_{24}$, >90%, TCI)) were injected as a last step of the injection before experiments started.

The concentration of HCs and CCl_4 were monitored using a Gas Chromatography–Flame Ionizer Detector (Agilent, model 7820A) (GC-FID). The HC concentration detected by GC–FID determined HC consumption in the chamber during the experiment. The concentration of CCl_4 measured by GC-FID was monitored as a function of time to obtain the dilution factor of the chamber during the experiment. The concentration of O_3 was monitored with a photometric ozone analyzer (Teledyne, model 400E and 2B Technologies, model 106-L, M). NO_x concentration was monitored by using a chemiluminescence NO/NO_2 analyzer (Teledyne, model 200E) and photometric NO_x analyzer (2B Technologies, model 405 nm). The inorganic ion (SO_4^{2-} and NH_4^+) and organic carbon (OC) concentrations of aerosol were in situ monitoring by the Particle-Into-Liquid-Sampler (Applikon, ADI 2081), coupled with Ion Chromatography (Metrohm, 761Compact IC) (PILS–IC), and an OC/EC carbon aerosol analyzer (Sunset Laboratory, Model 4), respectively. The Scanning Mobility Particle Sizer (SMPS, TSI, Model 3080) integrated with a condensation nuclei counter (TSI, Model 3025A and Model 3022) was used to measure the particle volume concentration over the course of experiment. An Aerosol Chemical Speciation Monitor (ACSM, Aerodyne Research Inc.) observed the composition (SO_4^{2-}, NO_3^-, NH_4^+, and organic) of aerosol to compare with the data obtained from OC and PILS–IC for the accurate measurement. The relative humidity and temperature were monitored in the UF-APHOR and applied to the simulation, and the sunlight intensity was measured by Total Ultraviolet Radiometer (EPLAB, TUVR). Aerosol acidity

https://doi.org/10.5194/acp-2022-327
Preprint. Discussion started: 24 May 2022

Atmospheric Chemistry and Physics Discussions

(mol/L of aerosol) was examined by Colorimetry integrated in the Reflectance UV–visible spectrometer (CRUV) (Li and Jang, 2012;Jang et al., 2020). The details of the experimental conditions are summarized in Table 1.

3 Model descriptions

In the model, the oxidation products from each biogenic HC were predicted by using explicit mechanisms for each oxidant (OH radicals, O_3, NO_3 radicals, and $O(^3P)$). The simulated gas products were classified into the 51 lumping species (i) according to their volatility and reactivity in aerosol phase. The stoichiometric coefficients (α_i) array and physicochemical parameters ($p^{\circ}_{L,i}$, MW_i, $O{:}C_i$, and HB_i) of the lumping species (i) were determined by the near-explicit gas mechanisms. In order to increase the suitability, the UNIPAR model was coupled with the conventional ozone mechanisms, such as SAPRC07TC as seen in Fig. 1 (UNIPAR-SAPRC). The UNIPAR-SAPRC model was simulated under the Dynamically Simple Model of Atmospheric Chemical Complexity (DSMACC) (Emmerson and Evans, 2009) integrated with the Kinetic PreProcessor (KPP) (Damian et al., 2002). The HC consumption obtained from SAPRC, α_i, and physicochemical parameters of lumping species (i) were then applied to produce SOA mass (OM_T) via gas–particle partitioning (OM_P) and heterogeneous reactions (OM_{AR}) in both organic and inorganic phases. For α-pinene and β-caryophyllene, the SOA formation in the presence of salted aqueous solution was simulated under the assumption of the liquid-liquid phase separation (LLPS) between the organic and inorganic phase. The simulation of this study is limited to LLPS and thus, the isoprene SOA formation in the presence of inorganic aerosol was excluded. The water content in isoprene SOA, which is very hydrophilic, was estimated with 1/3 of hygroscopicity of ammonium sulfate (Beardsley and Jang, 2016). The details of the UNIPAR model were described in the following sections.

3.1 Generation of lumping species from the Explicit Gas Mechanisms

The gas-phase oxidation of three biogenic HCs (isoprene, α-pinene, and β-caryophyllene) of this study was explicitly processed by using the Master Chemical Mechanism (MCM v3.3.1) (Saunders et al., 2003;Jenkin et al., 2012;Jenkin et al., 2015) to generate lumping species and their model parameters. Additionally, the recently identified oxidation mechanisms that can yield low volatile products were also integrated with MCM. For example, the Peroxy Radical Autoxidation Mechanism (PRAM) (Roldin et al., 2019) that forms the highly oxygenated organic molecule (HOM) (Molteni et al., 2019) and the accretion reaction to form ROOR from the RO_2 (Bates et al., 2022;Zhao et al., 2021) were added. Furthermore, the oxidation process of biogenic HCs by $O(^3P)$ (Paulson et al., 1992;Alvarado et al., 1998) was included to fulfill the oxidation mechanism in the current regional model. The additional mechanisms are shown in the Sect. S1.2. The oxidation-path dependent lumping parameters were generated by individually processing the reaction of biogenic HCs with four major oxidants (OH radicals, O_3, NO_3 radicals, and $O(^3P)$). After a biogenic HC is oxidized with individual oxidants, the further oxidation of the 1st generation product was allowed to react with any oxidant. For instance, the 1st generation ozonolysis products of biogenic HC can react with OH radicals or NO_3 radicals.

The resulting oxygenated products from explicit gas mechanism were classified into eight levels of the vapor pressure ($P^{\circ}_{L,i}$) (1–8: 10^{-8}, 10^{-6}, 10^{-5}, 10^{-4}, 10^{-3}, 10^{-2}, 10^{-1}, and 1 mmHg) and six levels of the aerosol–phase reactivity scale (R_i): very fast (VF), fast (F), medium (M), slow (S), partitioning only (P), and multi-alcohol (MA), as well as three additional reactive species (glyoxal, methylglyoxal, and epoxydiols). The physicochemical parameters ($p^{\circ}_{L,i}$, MW_i, $O{:}C_i$, and HB_i) of lumping species (i) are determined based on the group contribution (Stein and Brown, 1994) and unified into one array for each HC. $\alpha_i$for each oxidation pathway was estimated by the predetermined mathematical equation originated from the explicit mechanism as a function of HC/NO_x (ppbC/ppb) level and aging factor (f_A). f_A is calculated from the concentration of HC, RO_2, and HO_2 (Zhou et al., 2019). Additionally, the product distribution leading to α_i can be impacted by the ozone to NO_x ratio, particularly

https://doi.org/10.5194/acp-2022-327
Preprint. Discussion started: 24 May 2022

Atmospheric Chemistry and Physics Discussions

at nighttime. In our study, the predetermined mathematical equation to construct α_i at night was determined at the constant HC (ppb) to ozone (ppb) ratio as 0.25.

3.2 SOA growth via gas-particle partitioning

In this model, the gas–particle partitioning of oxidation products are assumed as an equilibrium partitioning process based on the absorptive partitioning theory (Pankow, 1994). It assumes that the gas–particle partitioning instantaneously reaches equilibrium to distribute the gas products into the gas ($C_{g,i}$), organic ($C_{or,i}$) and inorganic phases ($C_{in,i}$). The partitioning coefficient of *i* into the organic phase ($K_{or,i}$, m^3 μg^{-1}) is determined by the traditional absorptive partitioning theory (Pankow, 1994) as follows:

$$K_{or,i} = \frac{7.501RT}{10^9 MW_{or}\gamma_{or,i}p^{\circ}_{L,i}}, \quad (1)$$

where MW_{or} (g mol^{-1}) is the molecular weight of OM_T, R (8.314 J mol^{-1} K^{-1}) is the ideal gas constant, and T (K) is the temperature. $\gamma_{or,i}$ is the activity coefficient of *i* in organic phase and assumed as unity. The partitioning coefficient of *i* into the inorganic phase ($K_{in,i}$, m^3 μg^{-1}) is also calculated as the traditional absorptive partitioning theory:

$$K_{in,i} = \frac{7.501RT}{10^9 MW_{in}\gamma_{in,i}p^{\circ}_{L,i}}, \quad (2)$$

where MW_{in} (g mol^{-1}) is the averaged molecular weight of inorganic aerosol, and $\gamma_{in,i}$ is the activity coefficient of *i* in inorganic phase. Unlike $\gamma_{or,i}$, $\gamma_{in,i}$ is semiempirically estimated with a polynomial equation, determined by fitting the $\gamma_{in,i}$ estimated by the Aerosol Inorganic–Organic Mixtures Functional groups Activity Coefficient (AIOMFAC) (Zuend et al., 2011) as:

$$\gamma_{in,i} = e^{0.035MW_i - 2.704\ln(O:C_i) - 1.121HB_i - 0.33FS - 0.022(RH)}, \quad (3)$$

where RH and FS is relative humidity (%) and fractional sulfate. Fractional sulfate (FS) is the concentration ratio of total sulfate to the sum of total sulfate and ammonium ions in aerosol (FS = $[SO_4^{2-}]/([SO_4^{2-}]+[NH_4^+])$) (Zhou et al., 2019). FS, introduced to determine aerosol acidity, ranges from 0.33 to 1 for ammonium sulfate to sulfuric acid, respectively.

The gas–organic partitioning is governed by Raoult's law, assumed that the saturation vapor pressure of the species is dependent on the mole fraction of the species in the solution. To consider the oligomerization of organic species in total concentration ($C_{T,i} = C_{g,i} + C_{or,i} + C_{in,i}$), OM_P is recalculated after OM_{AR} integration with the partitioning model (Schell et al., 2001), which is reconstructed by including OM_{AR} (Cao and Jang, 2010). OM_P is calculated by the Newton Raphson method (Press et al., 1992) from $C_{T,i}$ using a mass balance equation:

$$OM_P = \sum_i [C_{T,i} - OM_{AR,i} - C^*_{g,i}\frac{\left(\frac{C_{or,i}}{MW_i}\right)}{\sum_i\left(\frac{C_{or,i}}{MW_i}+\frac{OM_{AR,i}}{MW_{oli,i}}\right)+OM_0}], \quad (4)$$

where OM_0 (mol m^{-3}), $C^*_{g,i}(=\frac{1}{K_{or,i}})$, and $MW_{oli,i}$ (g mol^{-1}) are the concentration of pre-existing OM, the effective saturation concentration of *i*, and the molecular weight of the dimer (*i*), respectively.

3.3 SOA formation via aerosol phase reaction

Organic matter (OM_{AR}) is generated via aerosol phase reaction in both organic and inorganic phases, as well as gas-particle partitioning (OM_P). OM_{AR} is estimated as a second order reaction product from condensed organics based on the assumption of a self-dimerization reaction of organic compounds in media (Im et al., 2014;Zhou et al., 2019;Odian, 2004):

$$\frac{dC'_{or,i}}{dt} = -k_{o,i}{C'_{or,i}}^2, \quad (5)$$

$$\frac{dC'_{in,i}}{dt} = -k_{AC,i}{C'_{in,i}}^2, \quad (6)$$

https://doi.org/10.5194/acp-2022-327
Preprint. Discussion started: 24 May 2022

Atmospheric Chemistry and Physics Discussions

where $C'_{or,i}$ and $C'_{in,i}$ are the concentration of i in the organic and inorganic aerosol phase (mol L^{-1}), respectively. The reaction rate constant in the aqueous phase ($k_{AC,i}$) and organic phase ($k_{o,i}$) are determined:

$$k_{AC,i} = 10^{0.25pK_{BH_i^+} + 1.0X + 0.95R_i + \log(a_w[H^+]) - 2.58}, \quad (7)$$

$$k_{o,i} = 10^{0.25pK_{BH_i^+} + 0.95R_i + 1.2\left(1 - \frac{1}{1+e^{0.05(300-MW_{or})}}\right) + \frac{2.2}{1+e^{6.0(0.75-O:C)}} - 10.07}, \quad (8)$$

where $k_{AC,i}$ (L mol^{-1} s^{-1}) is the second order rate constant which is a rate determining step for polymerization to form polyacetal (Jang et al., 2005;Jang et al., 2006). $k_{AC,i}$ is semiempirically determined from R_i, the protonation equilibrium constant ($pK_{BH_i^+}$), excess acidity (X) (Cox and Yates, 1979;Jang et al., 2006), water activity (a_w), and the proton concentration [H^+] (Im et al., 2014;Zhou et al., 2019). $k_{o,i}$ is determined by extrapolating $k_{AC,i}$ to the neutral condition in the absence of salted aqueous solution to process oligomerization in organic phase. $k_{o,i}$ is calculated without X, a_w, and [H^+] terms because a_w, [H^+], and X converged to zero in the absence of wet inorganic seed.

3.4 Integration of UNIPAR with SAPRC

In this study, the UNIPAR model was coupled with SAPRC07TC (UNIPAR-SAPRC) to yield the concentration of RO_2, HO_2, and HC as a function of time under the given conditions. RO_2 and HO_2 concentrations, and the consumptions of biogenic HCs by four different oxidation pathways were applied to the predetermined mathematical equations, established from explicit gas mechanism to estimate the concentration of lumping species produced from each oxidation pathways. The resulting concentration of lumping species are plugged into the UNIPAR model to simulate the SOA formation via the gas-particle partitioning and aerosol phase reaction. The reaction rate constant of β-caryophyllene in SAPRC07TC was adjusted based on that from the MCM mechanism (Jenkin et al., 2012). The resulting gas mechanism of biogenic HCs in SAPRC07TC was summarized in the Table S1.

For the SOA simulation with NO_3 radicals in the presence of wet inorganic seed aerosol, the heterogeneous hydrolysis of N_2O_5 was included in gas mechanisms. N_2O_5 forms via the equilibrium reaction of a NO_3 radical and NO_2 in gas phase but rapidly hydrolyzed by the interfacial process on the surface of salted aqueous aerosol to form nitric acid (Galib and Limmer, 2021).

4 Results and Discussions

4.1 Simulation of chamber data with the UNIPAR model

The predictability of the UNIPAR-SAPRC model was demonstrated by simulating SOA data obtained from the oxidation of three biogenic HCs (isoprene, α-pinene, and β-caryophyllene) in the UF-APHOR chamber under the various environmental conditions, such as NO_x level, inorganic seed conditions, and temperature in both day and night (Table 1).

Figure 2 shows the simulated total SOA mass (OM_T, solid line) and OM_P (dotted line) by the UNIPAR-SAPRC. The predicted SOA mass approached with four oxidation paths well accords with the observed SOA mass (symbol). For the ozonolysis of all three biogenic HCs of this study, OM_P attributes more to SOA formation in the presence of NO_x (Fig. 2 (b), (c), (e), (f), (h), and (j)) than in the absence of NO_x (Fig. 2 (a), (d), (g), and (i)). This suggests the importance of NO_3 radicals at nighttime. The SOA formation increased with wet inorganic seed due to aqueous phase reactions of reactive organic species, rendering the reduction of OM_P as seen in Fig. 2 (e and f). In the same manner, SOA formation with acidic seed increased but the fraction of OM_P of total SOA mass decreased (Fig. 2 (g)). However, in the presence of aqueous salts, NO_3 radicals rapidly react with NO_2 to form dinitrogen pentoxide (N_2O_5), which can undergo heterogeneous hydrolysis reaction on the surface of wet aerosol particles to form nitric acid (HNO_3) (Brown et al., 2006;Hu and Abbatt, 1997;Galib and Limmer, 2021). Thus, the seed effects

https://doi.org/10.5194/acp-2022-327
Preprint. Discussion started: 24 May 2022


Atmospheric Chemistry and Physics Discussions

observed in the presence of NO_x from the chamber-generated SOA was mainly attributed to the seed effect on the SOA formation form the ozonolysis products.

Figure 3 illustrates the chamber-generated SOA mass (symbol) under ambient sunlight, the simulated OM_T (solid line), and OM_P (dotted lines). The daytime simulation approached by the four oxidation paths with the UNIPAR-SAPRC model also well agreed with the SOA mass generated under various experimental conditions. For both isoprene SOA (Fig.3 (a) vs. (d)) and β-caryophyllene SOA (Fig. 3 (c) vs. (f)), a clear NO_x effect appeared for those performed under similar experimental conditions measurement and simulation during daytime, showing the higher SOA mass with the greater HC/NO_x level (lower NO_x) as previously reported in many studies (Carlton et al., 2009;Tasoglou and Pandis, 2015). The impact of acidic seed on α-pinene SOA formation (Fig. 3 (b) and (e)) was also simulated with the model as reported in other studies (Yu et al., 2021;Han et al., 2016;Kristensen et al., 2014). However, β-caryophyllene SOA was relatively insensitive to the aerosol acidity, which disagreed with the previous observations (Chan et al., 2011;Offenberg et al., 2009). The SOA yield from β-caryophyllene oxidation is very high, even in the absence of salted aqueous phase. Thus, the impact of aqueous reactions on β-caryophyllene can be less dramatic than that of α-pinene. In addition, the large molecules originating from β-caryophyllene oxidation might have a poor solubility in aqueous phase, weakening the impact of aerosol acidity on OM_{AR}.

4.2 Evaluation of Biogenic SOA Potential from Major Oxidation Paths

Figure 4 displays the potential SOA yield simulated by the UNIPAR-SAPRC model from each oxidation path, which is calculated with the same amount of HC consumption at two different NO_x levels ((a) high NO_x: HC/NO_x = 3 ppbC/ppb and (b) low NO_x: HC/NO_x = 10 ppbC/ppb). For this calculation, the consumptions of biogenic HCs are set to 50 ppb (138 μg m^{-3}), 30 ppb (162 μg m^{-3}), and 20 ppb (167 μg m^{-3}) for isoprene, α-pinene, and β-caryophyllene, respectively. The temperature is set to 298 K at two different relative humidity (RH) levels (45% and 80%) and three different seed conditions (no seed, wet-AS, and wet ammonium bisulfate (AHS)) with 10 μg m^{-3} of OM_0. For the inorganic seeded simulation, the seed concentration is 20 μg m^{-3} (dry mass). Overall, biogenic SOA formation from the $O(^3P)$ reaction path is absence in daytime.

In this study, the isoprene SOA in the presence of salted aqueous solution is excluded because the simulation focused on LLPS. Isoprene products are very polar and can be mixed with salted aqueous phase (Beardsley and Jang, 2016). Figure 4 shows that the efficient pathways to form isoprene SOA are the NO_3- and OH-initiated oxidation in both day and night. The nighttime SOA yield simulated with NO_3 radicals at the given condition of Fig. 4 is 12-17%. The contribution of NO_3 on SOA yields in daytime can possibly be minimal owing to the rapid photolysis of NO_3 (e.g., lifetime = 5s) (Magnotta and Johnston, 1980). The tendency of each oxidation path for isoprene SOA formation shown in Fig. 4 accords with the previous studies (Carlton et al., 2009;Kleindienst et al., 2007;Czoschke et al., 2003) in that the reaction with the OH radical mainly attributes to isoprene SOA. But the reaction with O_3 is a minor. Evidently, the SOA yield formed via ozonolysis in the absence of an OH-scavenger was greater than that in the presence of the scavenger in the laboratory work (Kleindienst et al., 2007), suggesting that a sizable fraction of the isoprene aerosol is produced via the OH-oxidation path.

The α-pinene SOA yields is high with ozonolysis and NO_3-initiated oxidation in both daytime and nighttime, due to the formation of lowly volatile products from the autoxidation of ozonolysis products (Roldin et al., 2019;Crounse et al., 2013;Bianchi et al., 2019). In general, the photodegradation of oxidation products lessens SOA yields in daytime. As seen in Fig. 4, the NO_3-initiated reaction of α-pinene produces a considerable amount of SOA under darkness. The addition of NO_3 to the alkene double bond of α-pinene is followed by the addition of an oxygen molecule to form an alkylperoxy radical that can lead to low-volatile peroxide accretion products (ROOR) (Hasan et al., 2021;Bates et al., 2022).

Unlike the diurnal pattern in isoprene and α-pinene SOA yields as shown in Fig. 4, that of β-caryophyllene SOA yield shows higher in daytime than in nighttime. Similar to isoprene and α-pinene products, β-caryophyllene products can be degraded via

https://doi.org/10.5194/acp-2022-327
Preprint. Discussion started: 24 May 2022


Atmospheric Chemistry and Physics Discussions

photolysis and shorten their carbon number. However, the molecular weight of β-caryophyllene oxidation products is generally much higher than that in isoprene or α-pinene products. Even after photodegradation of β-caryophyllene products, the product volatility is still low enough to significantly partition to the aerosol phase and heterogeneously form SOA. Under darkness, the β-caryophyllene SOA formation potential is the highest with ozonolysis, followed by the NO_3-initiated oxidation. At given simulation conditions in Fig. 4, the β-caryophyllene SOA yield ranges from 26% to 35% for the OH-initiated oxidation and 21-32% for ozonolysis. The SOA yields from the reaction of β-caryophyllene with OH radicals and O_3 are found in other laboratory studies (i.e., SOA yields with OH: 17-68%, those with O_3: 5-46%) (Chan et al., 2011;Jaoui et al., 2013;Tasoglou and Pandis, 2015).

Figure 4 also shows the SOA potentials at the two different NO_x levels for each oxidation path. Overall, the NO_3-initiated SOA yield drops in decreasing the NO_x level, because the RO_2 that forms via the reaction of biogenic HC with NO_3 radical followed by the addition of an oxygen molecule can react with HO_2 radicals to form organic hydroperoxide, which yields little SOA mass (Bates et al., 2022;Ng et al., 2008). At the low NO_x level, the oxidation of HCs with the OH radical tends to form a large amount of SOA mass. For α-pinene and β-caryophyllene, the low NO_x level increases reactive organic products and thus SOA grows rapidly via heterogeneous reactions. The OH-initiated isoprene SOA yields increases with reducing the NO_x level because of the formation of epoxy-diol at the low NO_x levels (Kroll et al., 2006). The SOA yields from ozonolysis of α-pinene decreases by increasing the NO_x level. The autoxidation path of the α-pinene ozonolysis product can be suppressed under the high NO_x level (Bianchi et al., 2019). Thus, it lowers the formation of low volatility products. For β-caryophyllene, the nighttime SOA formation from ozonolysis increases with reducing the NO_x level, because the internal rearrangement of ozonolysis products to form the secondary ozonide competes with the reaction of these ozonolysis products with NO or NO_2 (Jenkin et al., 2012). The further oxidation of the secondary ozonide products yield low-volatile products. However, the ozonolysis β-caryophyllene SOA under sunlight increases with increasing the NO_x level. The first generation of the ozonolysis of β-caryophyllene forms product containing an alkene double bond and an aldehyde group, which can react with a NO_3 radical to form high-carbon peroxy radicals. Furthermore, these peroxy radicals can produce a variety of organic products that form SOA via heterogeneous reactions and partitioning of the low volatility products (Jenkin et al., 2012;Li et al., 2011).

Regardless of HCs and oxidation pathways, the impact of neutral seed (wet-AS) on biogenic SOA formation is insignificant. The impact of the acidic seed (wet-AHS) on α-pinene SOA formation is various depending upon the oxidation path. For daytime SOA formation, the significant impact of acidic seed on SOA formation is observed as previously reported (Yu et al., 2021;Han et al., 2016). For nighttime, no significant impact of acid-catalyzed reactions on the α-pinene SOA originating from the NO_3-initiated pathway appears, because the SOA forms from lowly volatile ROOR products that are insensitive to aerosol acidity (Boyd et al., 2017). For β-caryophyllene, overall, the increase in SOA yields due to aqueous phase reactions are not significant for all oxidation pathways. Only a small increase in the β-caryophyllene SOA yield in the presence of acidic seed (wet-AHS) appears for the O_3-initiated oxidation path at nighttime and daytime.

The chamber-generated SOA mass is influenced by the deposition of organic vapor to the chamber wall. The simulation of SOA yields in Fig. 4 is performed with the model parameters obtained in the presence of the chamber wall. To investigate the SOA formation in the ambient air, the wall-free SOA model parameter has recently been derived by (Han and Jang, 2022). Figure S3 illustrates the SOA yields predicted in the absence of the deposition of organic vapor to the chamber wall. Overall, the effect of acidic seed on SOA formation is reduced by the correction of model parameters for the wall artifact. α-Pinene SOA is more influenced by gas-wall partitioning than isoprene or β-caryophyllene SOA, especially for the OH radical and NO_3 radical oxidation paths.

https://doi.org/10.5194/acp-2022-327
Preprint. Discussion started: 24 May 2022

Atmospheric Chemistry and Physics Discussions

4.3 Sensitivity of Biogenic SOA Formation to Major Variables

Figure 5 illustrates the simulated SOA yield from (a) isoprene, (b) α-pinene, and (c) β-caryophyllene in both daytime (solid line) and nighttime (dashed line) under the various temperature, ranging from 278K to 308K, at the given reference condition. The bias from gas-wall partitioning is corrected in this simulation by the amended model parameter (Han and Jang, 2022). For the daytime, the SOA formation is simulated under the reference sunlight intensity (Fig. S1), measured on 06/19/2015 at the UF-APHOR. The simulation is performed for the urban atmosphere where the NO_x level is high (HC/NO_x = 3 ppbC/ppb), because the concentration of O_3 and NO_3 radicals are relatively high in the polluted atmosphere. The SOA formation is simulated with 10 μg m^{-3} of OM_0 at the constant RH (50%) with the fixed initial concentration of isoprene, α-pinene, and β-caryophyllene as 50 ppb, 30 ppb, and 24 ppb, respectively. The sensitivity of SOA mass to temperature is simulated for α-pinene and β-caryophyllene under NS and wet-AHS (20 μg m^{-3}) conditions. The contribution of each oxidation pathway to the consumption of biogenic HC is illustrated in Fig. S2 (a).

Figure 5 shows that isoprene and α-pinene produce more SOA mass at nighttime than daytime. In Fig. S2 (a), more than 90% of isoprene and α-pinene are consumed by NO_3 radicals and O_3 at night, while they are mainly consumed by OH radicals in daytime. As discussed in Sect. 4.2, their oxidation paths with NO_3 radicals or O_3 at night produce considerably high SOA mass yields. For β-caryophyllene, the majority of HC is consumed by O_3 in both day and night. In addition, OH radicals' contribution to the HC consumption is positively correlated to the ozonolysis, which produces the OH radicals as a byproduct. The daytime SOA yield (Fig. S3) from the β-caryophyllene ozonolysis and OH-initiated oxidation are similar or greater than that in night due to the formation of reactive products for oligomerization during multi-generation photochemical oxidation as discussed in section 4.2.

In the absence of the inorganic seed, the nighttime SOA from all three HCs is more sensitive to the temperature than that produced in daytime. At nighttime, the biogenic HCs, primarily consumed by O_3 and NO_3 radicals, produce the semi-volatiles that form SOA dominantly by the partitioning process. The products formed via the photooxidation in daytime are multi-functional and reactive for aerosol phase reactions, and thus less sensitive to temperature.

The daytime α-pinene SOA formation is enhanced by the acid-catalyzed reaction up to 1.2 times (Fig. 5 (b)). However, the nighttime α-pinene SOA mass decreases by introducing inorganic seeds due to the decay of the NO_3 radicals through the heterogeneous hydrolysis of N_2O_5, which thermodynamically forms NO_3 radicals. The reduction of NO_3 radicals results in less contribution of the NO_3 path that can lead a high yield SOA formation (Fig. S3 (a)). In both nighttime and daytime, β-caryophyllene SOA mass increases up to 1.1 times by aqueous phase reactions. The impact of wet seed on isoprene SOA is not discussed in this study because the mixing state of isoprene products and wet-salt aerosol is not governed by LLPS. Studies have shown that the impact of aqueous reaction isoprene SOA is greater than α-pinene (Beardsley and Jang, 2016;Carlton et al., 2009).

Figure 6 illustrates the sensitivity of SOA yields to the NO_x level at a given reference condition with 10 μg m^{-3} of OM_0. The temperature and RH are set to 298 K and 50%, respectively. The simulations are performed in the absence of the gas-wall partitioning (Han and Jang, 2022) with the given initial concentration of isoprene, α-pinene, and β-caryophyllene as 50 ppb, 30 ppb, and 24 ppb, respectively. The SOA simulations from α-pinene and β-caryophyllene are performed under NS and wet-AHS conditions. The dry mass of wet-AHS is set to 20 μg m^{-3}. Figure 6 shows the impact of NO_x to ozonolysis SOA at nighttime. Despite of a large increase in α-pinene SOA potential due to the gas-wall loss correction (Fig. 4 vs. Fig. S3), the highest yield in daytime SOA appears with β-caryophyllene, followed by α-pinene and isoprene. In nighttime, the simulation suggests that α-pinene SOA yield could be higher than the β-caryophyllene SOA at the high NO_x zone due to the high SOA potential from the NO_3-initiated oxidation path.

https://doi.org/10.5194/acp-2022-327
Preprint. Discussion started: 24 May 2022


Atmospheric Chemistry and Physics Discussions

For α-pinene and isoprene, daytime SOA yields gradually decrease with increasing NO_x, but nighttime SOA yields drastically increase in the high NO_x region. In daytime, the high NO_x level increases the reactions of NO with RO_2, leading to relatively volatile gas products lowering SOA yields (Yu et al., 2021;Carlton et al., 2009;Hallquist et al., 2009). At night, as seen in Fig. S2, the high-yield NO_3-initiated path contributes more with the high NO_x level. The NO_x effects on nighttime biogenic SOA formation in the presence of inorganic seed are lesser than those in daytime due to the removal process of NO_3 radicals via the heterogeneous hydrolysis of N_2O_5 on the wet inorganic seed. For β-caryophyllene, the NO_x effects on SOA yield shows the opposite trend to α-pinene and isoprene SOA. The daytime β-caryophyllene SOA yields from ozonolysis decreases with reducing NO_x level. Figure S2 suggests that the β-caryophyllene is mainly consumed by the O_3 initiated path, and thus the β-caryophyllene SOA yield in daytime changes by NO_x level (Fig. S3) due to the different product distributions from the ozonolysis as discussed in section 4.2.

4.4 Nocturnal Biogenic SOA Formation in the Presence of gasoline

To investigate the influence of anthropogenic HC on the terpene SOA formation at night, 75 ppb α-pinene is oxidized with 120 ppb O_3 in the presence of 3000 ppbC gasoline fuel. The details of the experimental conditions are summarized in Table 2. Fig.7 illustrates the UNIPAR-SAPRC simulated SOA mass (OM_T, solid line) and the observed chamber-generated SOA mass (symbol). The aromatic HCs in gasoline fuel can be oxidized with the OH radicals, which is produced as a by-product from the ozonolysis of α-pinene (Finlayson-Pitts and Pitts Jr, 1999). The simulation suggests that the SOA formation in the α-pinene and gasoline cocktail mainly originates from α-pinene oxidation products. The α-pinene SOA (red line) contributes from 95 to 98% of total SOA in the absence of inorganic seed (Fig. 7 (a)), and it slightly decreases to 93-94% in the presence of wet-AS because the gasoline aromatic oxidation products are highly reactive in the aqueous phase (Han and Jang, 2022). The simulated α-pinene SOA mass in the presence of gasoline fuel is also compared to that in the absence of gasoline in Fig. 7. Interestingly, the SOA formation in the presence of gasoline is elevated by 30% compared to that in absence. Under the ozone excess condition of this study, the oxidation of α-pinene is mainly dominated by ozonolysis in the presence of gasoline, because gasoline competes with α-pinene to react with OH radicals. As seen in Fig. 4, α-pinene ozonolysis is capable of yielding higher SOA mass than the α-pinene OH reaction.

The impact of anthropogenic hydrocarbons (gasoline) on α-pinene SOA is also demonstrated for different NO_x levels and seed conditions without the chamber wall bias in Fig. S4. In the absence of inorganic seed, the simulation shows the higher SOA yields with the greater NO_3 contribution at the higher NO_x. In the presence of inorganic seed, the contribution of NO_3 on SOA formation decreases due to the heterogeneous hydrolysis of N_2O_5, which forms the NO_3 radicals as discussed in section 4.3. The effects of gasoline to total SOA formation decrease with increasing the NO_x level, because less ozonolysis results in less production of OH radicals. In addition, the aromatic SOA yield is generally smaller at the higher NO_x level (Han and Jang, 2022).

4.5 Impact of Model Parameters on SOA mass

The uncertainty test of SOA mass is performed for two major processes associated with partitioning (P_L) and aerosol phase reactions in both the organic phase and the aqueous phase (k_o, and k_{AC}) in the absence of chamber wall bias. The uncertainty in SOA mass in Fig. S5 is performed by increasing/decreasing P_L, k_o, and k_{AC} as a factor of 1.5/0.5, at the high NO_x level (HC/NO_x = 3 ppbC/ppb) with 10 μg m^{-3} of OM_0. The daytime SOA mass is simulated with the sunlight profile on 06/19/2015 near summer solstice (Fig. S1). Temperature and RH are set as 298K and 40%, respectively. The amount of both wet-AS and wet-AHS is fixed to 20 μg m^{-3} (dry mass). In the model, P_L was determined based on the group contribution (Stein and Brown, 1994) with the reported error as a factor of 1.45 (Zhao et al., 1999). k_{AC} was semi-empirically determined by correlating model compound data with the $[H^+]$ and liquid water contents, and R_i (Eq. 7). k_o was obtained by extending the k_{AC} calculation to

https://doi.org/10.5194/acp-2022-327
Preprint. Discussion started: 24 May 2022


Atmospheric Chemistry and Physics Discussions

the neutral condition in the absence of salted aqueous solution to process oligomerization in organic phase by eliminating X, a_w, and [H^+] terms (Eq. 8). Among the reaction systems in Fig. S5, α-pinene daytime SOA formation is the most responsive to the change of the three model parameters. P_L is more influential on all three biogenic SOA formation than k_o, and k_{AC} at the given simulation condition.

5 Atmospheric Implication

In this study, the biogenic SOA produced from the reaction of isoprene, α-pinene, or β-caryophyllene with four major atmospheric oxidants (OH radicals, O_3, NO_3 radicals, and $O(^3P)$) was simulated with the UNIPAR-SAPRC model and applied to interpretation of their diurnal pattern. The simulation (Fig. 6) indicated that isoprene and α-pinene SOA yields in daytime increased by decreasing the NO_x level, but they showed the opposite tendency at night. This trend accords with the previous laboratory studies and field observations (Rollins et al., 2012;Yu et al., 2021;Carlton et al., 2009;Hallquist et al., 2009;Fry et al., 2018). As seen in Fig. S2, the NO_3 radical significantly contributed to the biogenic HC consumption at night, although its contribution can be lesser in the presence of wet inorganic aerosol. Field observations have shown a considerable contribution of NO_3 radicals to biogenic HC oxidation at night, up to 58% of the total oxidation paths (Ng et al., 2017;Edwards et al., 2017).

Owing to the efforts of the governmental agency, the NO_x emission from anthropogenic sources has gradually decreased, and it impacts the NO_3 concentrations. For example, the nighttime oxidation path in the southeast US is in transition from NO_x-dominance to O_3-dominance (Edwards et al., 2017), due to the reduction of the NO_x emission (Russell et al., 2012). The fate of SOA formation caused by the nocturnal chemistry under the reduction of the NO_x emission is, however, complex due to several reasons. Under the urban set, the biogenic HCs are oxidized in the presence of the complex cocktail of anthropogenic pollutants (i.e., aromatic HCs, SO_2 and NO_x). As discussed in section 4.4, the reduction of NO_x can lessen biogenic SOA mass at night (Figure 4 and Figure 6), although it increases aromatic SOA originating from the oxidation with OH radical. On the other hand, the reduction of NO_x can increase daytime biogenic SOA burdens in urban air. Additionally, NO_2 can react with OH radicals at high NO_x zones to form HNO_3, which is semi-volatile and can condense onto the preexisting particles at the low temperature (Wang et al., 2020). Under the rural environment where the NO_x level is low, the reduction of NO_x can generally increase biogenic SOA formation in both daytime and nighttime, but its impact could be trivial compared to that in the high NO_x zone.

Electrolytic inorganic salts are ubiquitous in the urban air because sulfate and nitrate are produced by the atmospheric oxidation of SO_2 and NO_x, respectively (Finlayson-Pitts and Pitts Jr, 1999). For last two decades, numerous studies have shown the significant increase in biogenic SOA mass in the presence of acidic seed due to the acid-catalyzed heterogeneous reactions (Jang et al., 2002;Czoschke et al., 2003;Offenberg et al., 2009;Surratt et al., 2010;Beardsley and Jang, 2016;Hallquist et al., 2009). Most previous studies have demonstrated the impact of acidic aerosol on daytime SOA. In this study, both simulations and chamber observations (Figure 4) showed a weak seed impact on ozonolysis biogenic SOA. The nighttime biogenic SOA formation via the NO_3-initiated oxidation path was even less sensitive to the seed condition compared to ozonolysis SOA. Boyd et al. (2017) also reported a similar observation for monoterpenes (Boyd et al., 2017). In addition, the contribution of NO_3 radicals on nighttime SOA formation under the high NO_x zone can be less in the presence of salted aqueous solution. The heterogeneous hydrolysis of N_2O_5 (Brown et al., 2006;Hu and Abbatt, 1997) on the surface of inorganic seed lessens the concentration of NO_3 radicals. However, when nighttime SOA formation is dominated by ozonolysis at the low NO_x zone, the SOA formation can be enhanced by wet seed (Fig. S3).

The emission of biogenic HCs is regulated by temperature and light intensity (Holzke et al., 2006;Chen et al., 2020;Petron et al., 2001;Goldstein et al., 1998). Thus, there is a diurnal pattern in the biogenic HC emission, showing the higher biogenic HC emission during daytime (Holzke et al., 2006). The concentrations of O_3 and NO_2 are generally high at daytime due to the

https://doi.org/10.5194/acp-2022-327
Preprint. Discussion started: 24 May 2022


Atmospheric Chemistry and Physics Discussions

oxidation of hydrocarbon, involving the photochemical cycle of NO_x and the anthropogenic emission from human activities. The emission of biogenic HCs is lower by 3-4 times at night (Holzke et al., 2006) than that in daytime considering emission rate and the mixing height, but biogenic SOA yields significantly increase at night because of different oxidation paths and temperature reduction. For example, terpene and isoprene SOA yields increase almost by one order of magnitude as discussed in Fig. 5.

The model uncertainties to predict SOA mass mainly originates from gas mechanisms and aerosol phase reactions. The model approach by using explicit mechanisms is complex and time demanding, but it can improve a predictability of multiphase partitioning of products and heterogeneous reactions under varying environmental conditions. For example, the daytime β-caryophyllene SOA of this study was underpredicted as seen in Fig. 3, suggesting that the improvement of explicit gas mechanisms is essential to better predict SOA formation. In the model, the multiphase reaction of biogenic HC is individually treated with four different oxidation paths. Neither complex cross reactions between RO_2 radicals nor the long-term aging process of multiple generation products were not fully considered, which can be a source of the bias in SOA prediction. In the presence of inorganic seed, heterogenous hydrolysis of N_2O_5 was assumed to be very rapid. However, the variation of aerosol constituents can influence the accommodation coefficient of N_2O_5. For example, the heterogeneous hydrolysis of N_2O_5 on organic-coated aerosol can be slower than that in salted aqueous phase (Anttila et al., 2006). To accurately model the reaction of biogenic HCs with NO_3 radicals, the impact of aerosol compositions on the heterogeneous reaction of N_2O_5 on the surface of aerosol needs to be investigated in future. In addition, the hydrolysis of organonitrates in aerosol phase and the aging of particle organic matter were not included in the model.

Code availability. Code to run the SOA model in this study is available upon request.

Data availability. The chamber data and simulated results used in this study are available upon request.

Author contribution. MJ and SH designed the experiments, and SH carried them out. SH prepared the manuscript with contributions from MJ.

Competing interest. The authors declare that neither they nor their co-author has any conflict of interest.

Acknowledgments. This research was supported by the National Institute of Environmental Research (NIER2020-01-01-010); the National Science Foundation (AGS1923651); and the Fine Particle Research Initiative in East Asia Considering National Differences (FRIEND) Project through the National Research Foundation of Korea (NRF) funded by the Ministry of Science and ICT (2020M3G1A1114556).

https://doi.org/10.5194/acp-2022-327
Preprint. Discussion started: 24 May 2022

Atmospheric Chemistry and Physics Discussions

References

Altieri, K. E., Carlton, A. G., Lim, H.-J., Turpin, B. J., and Seitzinger, S. P.: Evidence for oligomer formation in clouds: Reactions of isoprene oxidation products, Environmental science & technology, 40, 4956-4960, 2006.

Alvarado, A., Tuazon, E. C., Aschmann, S. M., Atkinson, R., and Arey, J.: Products of the gas-phase reactions of O (3 P) atoms and O3 with α-pinene and 1, 2-dimethyl-1-cyclohexene, Journal of Geophysical Research: Atmospheres, 103, 25541-25551, 1998.

Anttila, T., Kiendler-Scharr, A., Tillmann, R., and Mentel, T. F.: On the reactive uptake of gaseous compounds by organic-coated aqueous aerosols: Theoretical analysis and application to the heterogeneous hydrolysis of N2O5, The Journal of Physical Chemistry A, 110, 10435-10443, 2006.

Atkinson, R., and Arey, J.: Atmospheric degradation of volatile organic compounds, Chemical reviews, 103, 4605-4638, 2003.

Barnes, I., Bastian, V., Becker, K. H., and Tong, Z.: Kinetics and products of the reactions of nitrate radical with monoalkenes, dialkenes, and monoterpenes, Journal of Physical Chemistry, 94, 2413-2419, 1990.

Barreira, L. M., Ylisirniö, A., Pullinen, I., Buchholz, A., Li, Z., Lipp, H., Junninen, H., Hõrrak, U., Noe, S. M., and Krasnova, A.: The importance of sesquiterpene oxidation products for secondary organic aerosol formation in a springtime hemiboreal forest, Atmospheric Chemistry and Physics, 21, 11781-11800, 2021.

Bates, K. H., Burke, G. J., Cope, J. D., and Nguyen, T. B.: Secondary organic aerosol and organic nitrogen yields from the nitrate radical (NO 3) oxidation of alpha-pinene from various RO 2 fates, Atmospheric Chemistry and Physics, 22, 1467-1482, 2022.

Beardsley, R., and Jang, M.: Simulating the SOA formation of isoprene from partitioning and aerosol phase reactions in the presence of inorganics, Atmospheric Chemistry and Physics, 16, 5993-6009, 10.5194/acp-16-5993-2016, 2016.

Bianchi, F., Kurten, T., Riva, M., Mohr, C., Rissanen, M., Roldin, P., Berndt, T., Crounse, J., Wennberg, P., Mentel, T., Wildt, J., Junninen, H., Jokinen, T., Kulmala, M., Worsnop, D., Thornton, J., Donahue, N., Kjaergaard, H., and Ehn, M.: Highly Oxygenated Organic Molecules (HOM) from Gas-Phase Autoxidation Involving Peroxy Radicals: A Key Contributor to Atmospheric Aerosol, Chemical Reviews, 119, 3472-3509, 10.1021/acs.chemrev.8b00395, 2019.

Bonn, B., and Moorgat, G.: New particle formation during a-and b-pinene oxidation by O 3, OH and NO 3, and the influence of water vapour: particle size distribution studies, Atmospheric Chemistry and Physics, 2, 183-196, 2002.

Boyd, C. M., Nah, T., Xu, L., Berkemeier, T., and Ng, N. L.: Secondary organic aerosol (SOA) from nitrate radical oxidation of monoterpenes: effects of temperature, dilution, and humidity on aerosol formation, mixing, and evaporation, Environmental science & technology, 51, 7831-7841, 2017.

Brown, S., Ryerson, T., Wollny, A., Brock, C., Peltier, R., Sullivan, A., Weber, R., Dube, W., Trainer, M., and Meagher, J. F.: Variability in nocturnal nitrogen oxide processing and its role in regional air quality, Science, 311, 67-70, 2006.

Cao, G., and Jang, M.: An SOA model for toluene oxidation in the presence of inorganic aerosols, Environmental science & technology, 44, 727-733, 2010.

Carlton, A., Wiedinmyer, C., and Kroll, J.: A review of Secondary Organic Aerosol (SOA) formation from isoprene, 2009.

Chan, M., Surratt, J., Chan, A., Schilling, K., Offenberg, J., Lewandowski, M., Edney, E., Kleindienst, T., Jaoui, M., and Edgerton, E.: Influence of aerosol acidity on the chemical composition of secondary organic aerosol from β-caryophyllene, Atmospheric Chemistry and Physics, 11, 1735-1751, 2011.

Chen, J., Tang, J., and Yu, X.: Environmental and physiological controls on diurnal and seasonal patterns of biogenic volatile organic compound emissions from five dominant woody species under field conditions, Environmental Pollution, 259, 113955, 2020.

Cox, R. A., and Yates, K.: Kinetic equations for reactions in concentrated aqueous acids based on the concept of" excess acidity", Canadian Journal of Chemistry, 57, 2944-2951, 1979.

Crounse, J. D., Nielsen, L. B., Jørgensen, S., Kjaergaard, H. G., and Wennberg, P. O.: Autoxidation of organic compounds in the atmosphere, The Journal of Physical Chemistry Letters, 4, 3513-3520, 2013.

Czoschke, N. M., Jang, M., and Kamens, R. M.: Effect of acidic seed on biogenic secondary organic aerosol growth, Atmospheric Environment, 37, 4287-4299, 2003.

Damian, V., Sandu, A., Damian, M., Potra, F., and Carmichael, G. R.: The kinetic preprocessor KPP-a software environment for solving chemical kinetics, Computers & Chemical Engineering, 26, 1567-1579, 2002.

Donahue, N., Robinson, A., Stanier, C., and Pandis, S.: Coupled partitioning, dilution, and chemical aging of semivolatile organics, Environmental Science & Technology, 40, 2635-2643, 10.1021/es052297c, 2006.

Edwards, P., Aikin, K., Dube, W., Fry, J., Gilman, J., De Gouw, J., Graus, M., Hanisco, T., Holloway, J., and Hübler, G.: Transition from high-to low-NOx control of night-time oxidation in the southeastern US, Nature Geoscience, 10, 490-495, 2017.

Emmerson, K., and Evans, M.: Comparison of tropospheric gas-phase chemistry schemes for use within global models, Atmospheric Chemistry & Physics, 9, 2009.

Ervens, B., Feingold, G., Frost, G. J., and Kreidenweis, S. M.: A modeling study of aqueous production of dicarboxylic acids: 1. Chemical pathways and speciated organic mass production, Journal of Geophysical Research: Atmospheres, 109, 2004.

Finlayson-Pitts, B. J., and Pitts Jr, J. N.: Chemistry of the upper and lower atmosphere: theory, experiments, and applications, Elsevier, 1999.

Fry, J. L., Brown, S. S., Middlebrook, A. M., Edwards, P. M., Campuzano-Jost, P., Day, D. A., Jimenez, J. L., Allen, H. M., Ryerson, T. B., and Pollack, I.: Secondary organic aerosol (SOA) yields from NO 3 radical+ isoprene based on nighttime aircraft power plant plume transects, Atmospheric Chemistry and Physics, 18, 11663-11682, 2018.

Galib, M., and Limmer, D. T.: Reactive uptake of N2O5 by atmospheric aerosol is dominated by interfacial processes, Science, 371, 921-925, 2021.

https://doi.org/10.5194/acp-2022-327
Preprint. Discussion started: 24 May 2022

Goldstein, A. H., Goulden, M. L., Munger, J. W., Wofsy, S. C., and Geron, C. D.: Seasonal course of isoprene emissions from a midlatitude deciduous forest, Journal of Geophysical Research: Atmospheres, 103, 31045-31056, 1998.

Goldstein, A. H., and Galbally, I. E.: Known and unexplored organic constituents in the earth's atmosphere, Environmental science & technology, 41, 1514-1521, 2007.

Guenther, A., Hewitt, C. N., Erickson, D., Fall, R., Geron, C., Graedel, T., Harley, P., Klinger, L., Lerdau, M., and McKay, W.: A global model of natural volatile organic compound emissions, Journal of Geophysical Research: Atmospheres, 100, 8873-8892, 1995.

Hallquist, M., Wenger, J., Baltensperger, U., Rudich, Y., Simpson, D., Claeys, M., Dommen, J., Donahue, N., George, C., Goldstein, A., Hamilton, J., Herrmann, H., Hoffmann, T., Iinuma, Y., Jang, M., Jenkin, M., Jimenez, J., Kiendler-Scharr, A., Maenhaut, W., McFiggans, G., Mentel, T., Monod, A., Prevot, A., Seinfeld, J., Surratt, J., Szmigielski, R., and Wildt, J.: The formation, properties and impact of secondary organic aerosol: current and emerging issues, Atmospheric Chemistry and Physics, 9, 5155-5236, 10.5194/acp-9-5155-2009, 2009.

Han, S., and Jang, M.: Prediction of secondary organic aerosol from the multiphase reaction of gasoline vapor by using volatility–reactivity base lumping, Atmospheric Chemistry and Physics, 22, 625-639, 2022.

Han, Y., Stroud, C. A., Liggio, J., and Li, S.-M.: The effect of particle acidity on secondary organic aerosol formation from α-pinene photooxidation under atmospherically relevant conditions, Atmospheric Chemistry and Physics, 16, 13929-13944, 2016.

Hasan, G., Valiev, R. R., Salo, V.-T., and Kurtén, T.: Computational Investigation of the Formation of Peroxide (ROOR) Accretion Products in the OH-and NO3-Initiated Oxidation of α-Pinene, The Journal of Physical Chemistry A, 125, 10632-10639, 2021.

Holzke, C., Hoffmann, T., Jaeger, L., Koppmann, R., and Zimmer, W.: Diurnal and seasonal variation of monoterpene and sesquiterpene emissions from Scots pine (Pinus sylvestris L.), Atmospheric Environment, 40, 3174-3185, 2006.

Hu, J., and Abbatt, J.: Reaction probabilities for N2O5 hydrolysis on sulfuric acid and ammonium sulfate aerosols at room temperature, The Journal of Physical Chemistry A, 101, 871-878, 1997.

Im, Y., Jang, M., and Beardsley, R.: Simulation of aromatic SOA formation using the lumping model integrated with explicit gas-phase kinetic mechanisms and aerosol-phase reactions, Atmospheric Chemistry & Physics, 14, 2014.

Jang, M., Czoschke, N., Lee, S., and Kamens, R.: Heterogeneous atmospheric aerosol production by acid-catalyzed particle-phase reactions, Science, 298, 814-817, 10.1126/science.1075798, 2002.

Jang, M., Czoschke, N. M., and Northcross, A. L.: Semiempirical model for organic aerosol growth by acid-catalyzed heterogeneous reactions of organic carbonyls, Environmental science & technology, 39, 164-174, 2005.

Jang, M., Czoschke, N. M., Northcross, A. L., Cao, G., and Shaof, D.: SOA formation from partitioning and heterogeneous reactions: model study in the presence of inorganic species, Environmental science & technology, 40, 3013-3022, 2006.

Jang, M., Sun, S., Winslow, R., Han, S., and Yu, Z.: In situ aerosol acidity measurements using a UV–Visible micro-spectrometer and its application to the ambient air, Aerosol Science and Technology, 54, 446-461, 2020.

Jaoui, M., Kleindienst, T. E., Docherty, K. S., Lewandowski, M., and Offenberg, J. H.: Secondary organic aerosol formation from the oxidation of a series of sesquiterpenes: α-cedrene, β-caryophyllene, α-humulene and α-farnesene with O3, OH and NO3 radicals, Environmental Chemistry, 10, 178-193, 2013.

Jenkin, M., Wyche, K., Evans, C., Carr, T., Monks, P., Alfarra, M., Barley, M., McFiggans, G., Young, J., and Rickard, A.: Development and chamber evaluation of the MCM v3.2 degradation scheme for beta-caryophyllene, Atmospheric Chemistry and Physics, 12, 5275-5308, 10.5194/acp-12-5275-2012, 2012.

Jenkin, M., Young, J., and Rickard, A.: The MCM v3. 3.1 degradation scheme for isoprene, Atmospheric Chemistry and Physics, 15, 11433-11459, 2015.

Jimenez, J. L., Canagaratna, M., Donahue, N., Prevot, A., Zhang, Q., Kroll, J. H., DeCarlo, P. F., Allan, J. D., Coe, H., and Ng, N.: Evolution of organic aerosols in the atmosphere, Science, 326, 1525-1529, 2009.

Kanakidou, M., Seinfeld, J., Pandis, S., Barnes, I., Dentener, F. J., Facchini, M. C., Van Dingenen, R., Ervens, B., Nenes, A., and Nielsen, C.: Organic aerosol and global climate modelling: a review, Atmospheric Chemistry and Physics, 5, 1053-1123, 2005.

Kelly, J. M., Doherty, R. M., O'Connor, F. M., and Mann, G. W.: The impact of biogenic, anthropogenic, and biomass burning volatile organic compound emissions on regional and seasonal variations in secondary organic aerosol, Atmospheric Chemistry and Physics, 18, 7393-7422, 2018.

Kleindienst, T. E., Lewandowski, M., Offenberg, J. H., Jaoui, M., and Edney, E. O.: Ozone-isoprene reaction: Re-examination of the formation of secondary organic aerosol, Geophysical Research Letters, 34, 2007.

Kristensen, K., Cui, T., Zhang, H., Gold, A., Glasius, M., and Surratt, J.: Dimers in α-pinene secondary organic aerosol: effect of hydroxyl radical, ozone, relative humidity and aerosol acidity, Atmospheric Chemistry and Physics, 14, 4201-4218, 2014.

Kroll, J. H., Ng, N. L., Murphy, S. M., Flagan, R. C., and Seinfeld, J. H.: Secondary organic aerosol formation from isoprene photooxidation, Environmental science & technology, 40, 1869-1877, 2006.

Kwok, E. S., Aschmann, S. M., Arey, J., and Atkinson, R.: Product formation from the reaction of the NO3 radical with isoprene and rate constants for the reactions of methacrolein and methyl vinyl ketone with the NO3 radical, International Journal of Chemical Kinetics, 28, 925-934, 1996.

Li, J., and Jang, M.: Aerosol acidity measurement using colorimetry coupled with a reflectance UV-visible spectrometer, Aerosol Science and Technology, 46, 833-842, 2012.

Li, Y., Chen, Q., Guzman, M., Chan, C. K., and Martin, S.: Second-generation products contribute substantially to the particle-phase organic material produced by β-caryophyllene ozonolysis, Atmospheric Chemistry and Physics, 11, 121-132, 2011.

https://doi.org/10.5194/acp-2022-327
Preprint. Discussion started: 24 May 2022

Atmospheric Chemistry and Physics Discussions

Liggio, J., Li, S.-M., and McLaren, R.: Heterogeneous reactions of glyoxal on particulate matter: Identification of acetals and sulfate esters, Environmental science & technology, 39, 1532-1541, 2005.

Magnotta, F., and Johnston, H. S.: Photodissociation quantum yields for the NO3 free radical, Geophysical Research Letters, 7, 769-772, 1980.

Mauderly, J. L., and Chow, J. C.: Health effects of organic aerosols, Inhalation toxicology, 20, 257-288, 2008.

Molteni, U., Simon, M., Heinritzi, M., Hoyle, C. R., Bernhammer, A.-K., Bianchi, F., Breitenlechner, M., Brilke, S., Dias, A., and Duplissy, J.: Formation of highly oxygenated organic molecules from α-pinene ozonolysis: chemical characteristics, mechanism, and kinetic model development, ACS Earth and Space Chemistry, 3, 873-883, 2019.

Ng, N., Kwan, A., Surratt, J., Chan, A., Chhabra, P., Sorooshian, A., Pye, H. O., Crounse, J., Wennberg, P., and Flagan, R.: Secondary organic aerosol (SOA) formation from reaction of isoprene with nitrate radicals (NO 3), Atmospheric Chemistry and Physics, 8, 4117-4140, 2008.

Ng, N. L., Brown, S. S., Archibald, A. T., Atlas, E., Cohen, R. C., Crowley, J. N., Day, D. A., Donahue, N. M., Fry, J. L., and Fuchs, H.: Nitrate radicals and biogenic volatile organic compounds: oxidation, mechanisms, and organic aerosol, Atmospheric chemistry and physics, 17, 2103-2162, 2017.

Odian, G.: Principles of polymerization, John Wiley & Sons, 2004.

Odum, J., Hoffmann, T., Bowman, F., Collins, D., Flagan, R., and Seinfeld, J.: Gas/particle partitioning and secondary organic aerosol yields, Environmental Science & Technology, 30, 2580-2585, 10.1021/es950943+, 1996.

Offenberg, J. H., Lewandowski, M., Edney, E. O., Kleindienst, T. E., and Jaoui, M.: Influence of aerosol acidity on the formation of secondary organic aerosol from biogenic precursor hydrocarbons, Environmental science & technology, 43, 7742-7747, 2009.

Pankow, J. F.: An absorption model of the gas/aerosol partitioning involved in the formation of secondary organic aerosol, Atmospheric Environment, 28, 189-193, 1994.

Paulson, S. E., Flagan, R. C., and Seinfeld, J. H.: Atmospheric photooxidation of isoprene part I: The hydroxyl radical and ground state atomic oxygen reactions, International Journal of Chemical Kinetics, 24, 79-101, 1992.

Petron, G., Harley, P., Greenberg, J., and Guenther, A.: Seasonal temperature variations influence isoprene emission, Geophysical Research Letters, 28, 1707-1710, 2001.

Press, W. H., Teukolsky, S. A., Flannery, B. P., and Vetterling, W. T.: Numerical recipes in Fortran 77: volume 1, volume 1 of Fortran numerical recipes: the art of scientific computing, Cambridge university press, 1992.

Pye, H. O., Appel, K. W., Seltzer, K. M., Ward-Caviness, C. K., and Murphy, B. N.: Human-Health Impacts of Controlling Secondary Air Pollution Precursors, Environmental Science & Technology Letters, 2022.

Roldin, P., Ehn, M., Kurtén, T., Olenius, T., Rissanen, M. P., Sarnela, N., Elm, J., Rantala, P., Hao, L., and Hyttinen, N.: The role of highly oxygenated organic molecules in the Boreal aerosol-cloud-climate system, Nature communications, 10, 1-15, 2019.

Rollins, A. W., Browne, E. C., Min, K.-E., Pusede, S. E., Wooldridge, P. J., Gentner, D. R., Goldstein, A. H., Liu, S., Day, D. A., and Russell, L. M.: Evidence for NO x control over nighttime SOA formation, Science, 337, 1210-1212, 2012.

Russell, A., Valin, L., and Cohen, R.: Trends in OMI NO 2 observations over the United States: effects of emission control technology and the economic recession, Atmospheric Chemistry and Physics, 12, 12197-12209, 2012.

Sakulyanontvittaya, T., Guenther, A., Helmig, D., Milford, J., and Wiedinmyer, C.: Secondary organic aerosol from sesquiterpene and monoterpene emissions in the United States, Environmental science & technology, 42, 8784-8790, 2008.

Saunders, S. M., Jenkin, M. E., Derwent, R., and Pilling, M.: Protocol for the development of the Master Chemical Mechanism, MCM v3 (Part A): tropospheric degradation of non-aromatic volatile organic compounds, Atmospheric Chemistry and Physics, 3, 161-180, 2003.

Schell, B., Ackermann, I. J., Hass, H., Binkowski, F. S., and Ebel, A.: Modeling the formation of secondary organic aerosol within a comprehensive air quality model system, Journal of Geophysical Research: Atmospheres, 106, 28275-28293, 2001.

Sindelarova, K., Granier, C., Bouarar, I., Guenther, A., Tilmes, S., Stavrakou, T., Müller, J.-F., Kuhn, U., Stefani, P., and Knorr, W.: Global data set of biogenic VOC emissions calculated by the MEGAN model over the last 30 years, Atmospheric Chemistry and Physics, 14, 9317-9341, 2014.

Stein, S., and Brown, R.: Estimation of normal boiling points from group contributions, Journal of Chemical Information and Computer Sciences, 34, 581-587, 10.1021/ci00019a016, 1994.

Surratt, J. D., Chan, A. W., Eddingsaas, N. C., Chan, M., Loza, C. L., Kwan, A. J., Hersey, S. P., Flagan, R. C., Wennberg, P. O., and Seinfeld, J. H.: Reactive intermediates revealed in secondary organic aerosol formation from isoprene, Proceedings of the National Academy of Sciences, 107, 6640-6645, 2010.

Tasoglou, A., and Pandis, S.: Formation and chemical aging of secondary organic aerosol during the β-caryophyllene oxidation, Atmospheric Chemistry and Physics, 15, 6035-6046, 2015.

Tsigaridis, K., and Kanakidou, M.: The present and future of secondary organic aerosol direct forcing on climate, Current Climate Change Reports, 4, 84-98, 2018.

Wang, M., Kong, W., Marten, R., He, X.-C., Chen, D., Pfeifer, J., Heitto, A., Kontkanen, J., Dada, L., and Kürten, A.: Rapid growth of new atmospheric particles by nitric acid and ammonia condensation, Nature, 581, 184-189, 2020.

Woo, J. L., Kim, D. D., Schwier, A. N., Li, R., and McNeill, V. F.: Aqueous aerosol SOA formation: impact on aerosol physical properties, Faraday Discussions, 165, 357-367, 2013.

Yu, Z., Jang, M., Zhang, T., Madhu, A., and Han, S.: Simulation of Monoterpene SOA Formation by Multiphase Reactions Using Explicit Mechanisms, ACS Earth and Space Chemistry, 2021.

Zhang, H., Yee, L. D., Lee, B. H., Curtis, M. P., Worton, D. R., Isaacman-VanWertz, G., Offenberg, J. H., Lewandowski, M.,

https://doi.org/10.5194/acp-2022-327
Preprint. Discussion started: 24 May 2022

655 Kleindienst, T. E., and Beaver, M. R.: Monoterpenes are the largest source of summertime organic aerosol in the southeastern United States, Proceedings of the National Academy of Sciences, 115, 2038-2043, 2018.

Zhao, D., Pullinen, I., Fuchs, H., Schrade, S., Wu, R., Acir, I.-H., Tillmann, R., Rohrer, F., Wildt, J., and Guo, Y.: Highly oxygenated organic molecule (HOM) formation in the isoprene oxidation by NO 3 radical, Atmospheric Chemistry and Physics, 21, 9681-9704, 2021.

660 Zhao, L., Li, P., and Yalkowsky, S.: Predicting the entropy of boiling for organic compounds, Journal of Chemical Information and Computer Sciences, 39, 1112-1116, 10.1021/ci990054w, 1999.

Zhou, C., Jang, M., and Yu, Z.: Simulation of SOA formation from the photooxidation of monoalkylbenzenes in the presence of aqueous aerosols containing electrolytes under various NO x levels, Atmospheric Chemistry and Physics, 19, 5719-5735, 2019.

665 Zuend, A., Marcolli, C., Booth, A., Lienhard, D. M., Soonsin, V., Krieger, U., Topping, D. O., McFiggans, G., Peter, T., and Seinfeld, J. H.: New and extended parameterization of the thermodynamic model AIOMFAC: calculation of activity coefficients for organic-inorganic mixtures containing carboxyl, hydroxyl, carbonyl, ether, ester, alkenyl, alkyl, and aromatic functional groups, Atmospheric Chemistry and Physics, 11, 9155-9206, 2011.

670

https://doi.org/10.5194/acp-2022-327
Preprint. Discussion started: 24 May 2022

Atmospheric Chemistry and Physics Discussions

Tables and Figures

Table 1. Experimental conditions for the oxidation of biogenic HCs in the UF-APHOR chamber.

Exp. ID	Date	Initial condition					Temp (K)	%RH	max OM (μg m^{-3})	Light condition[4]	Figures
		HC (ppbC)	HC/NO_x (ppbC/ppb)	Seed[1]	Seed mass[2] (μg m^{-3})	OM_0[3] (μg m^{-3})					
Isoprene (C_5H_8)											
IS01	10/04/2021	750	-	-		5	295-302	44-81	27	N	Fig. 2 (a)
IS02	10/07/2021	782	13.3	-		5	297-301	42-56	31	N	Fig. 2 (b)
IS03	10/20/2021	750	3.9	-		5	292-298	36-75	30	N	Fig. 2 (c)
IS04	12/16/2021	696	5.6	-		5	291-310	16-38	116	Y	Fig. 3 (a)
IS05	01/27/2015	839	17.4	-		3	279-298	27-66	62	Y	Fig. 3 (d)
α-pinene ($C_{10}H_{16}$)											
AP01	03/19/2021	84	-	-		4	282-306	42-95	157	N	Fig. 2 (d)
AP02	06/23/2021	92	-	SA	100	4	296-899	72-88	96	N	Fig. 2 (e)
AP03	06/23/2021	79	-	wAS	100	4	296-300	89-100	80	N	Fig. 2 (e)
AP04	09/09/2021	64	10.5	-		5	296-299	34-42	37	N	Fig. 2 (f)
AP05	09/09/2021	58	10.5	SA	85	5	297-299	41-72	27	N	Fig. 2 (f)
AP06	09/20/2021	61	3.7	-		6	297-301	37-55	28	N	Fig. 2 (g)
AP07	09/20/2021	59	4.1	SA	87	6	298-302	37-55	33	N	Fig. 2 (g)
AP08	11/04/2021	60	2.3	dAS	40	5	288-294	32-45	58	N	Fig. 2 (h)
AP09	11/04/2021	60	2.3	-		5	289-293	44-66	63	N	Fig. 2 (h)
AP10	08/28/2019	124	11.3	-		4	296-320	14-40	23	Y	Fig. 3 (b)
AP11	08/28/2019	130	10.7	SA	50	4	296-317	32-54	98	Y	Fig. 3 (b)
AP12	07/18/2019	142	4.9	SA	60	3	294-320	13-42	52	Y	Fig. 3 (e)
AP13	07/18/2019	139	4.6	-		3	294-319	19-48	28	Y	Fig. 3 (e)
β-caryophyllene ($C_{15}H_{24}$)											
BC01	11/10/2021	50				4	292-299	29-67	95	N	Fig. 2 (i)
BC02	11/10/2021	50		SA	70	4	293-298	36-72	73	N	Fig. 2 (i)
BC03	11/23/2021	40	4.2			3	278-293	40-72	65	N	Fig. 2 (j)
BC04	12/03/2021	50	10.5	SA	120	3	281-308	23-90	219	Y	Fig. 3 (c)
BC05	12/03/2021	50	10.5			4	282-308	30-95	256	Y	Fig. 3 (c)
BC06	12/10/2021	50	3.8			3	287-310	25-77	100	Y	Fig. 3 (f)
BC07	12/10/2021	50	3.8	SA	150	3	288-311	26-72	87	Y	Fig. 3 (f)

[1]NS, SA, wAS, and dAS indicate non-seeded, sulfuric acid seed, wet ammonium sulfate seed, and dry ammonium sulfate seed, respectively. [2]The seed mass is determined as a dry mass, without water mass. [3]The pre-existing organic matter (OM_0) is determined for the chamber air prior to the injection of inorganic seed and HC. [4]Sunlight indicates the light condition of the experiment. N denotes the nighttime experiment conducted with no sunlight, and Y denotes the daytime experiments performed under the sunlight with photolysis.

https://doi.org/10.5194/acp-2022-327
Preprint. Discussion started: 24 May 2022

Atmospheric Chemistry and Physics Discussions

Table 2. Experimental conditions for the oxidation of α-pinene with gasoline fuel in the UF-APHOR chamber.

Exp. ID	Date	Initial condition						Temp (K)	%RH	max OM (μg m^{-3})
		α-pinene (ppbC)	Gasoline fuel (ppbC)	Seed[1]	O_3 (ppb)	Seed mass[2] (μg m^{-3})	OM_0[3] (μg m^{-3})			
APGF01	11/30/2021	750	3000	-	120		5	279-295	29-76	140
APGF02	11/30/2021	782	3000	wAS	115	94	5	279-296	38-89	120

[1]NS, SA, wAS, and dAS indicate non-seeded, sulfuric acid seed, wet ammonium sulfate seed, and dry ammonium sulfate seed, respectively. [2]The seed mass is determined as a dry mass, without water mass. [3]The pre-existing organic matter (OM_0) is determined for the chamber air prior to the injection of inorganic seed and HC.

685

https://doi.org/10.5194/acp-2022-327
Preprint. Discussion started: 24 May 2022

Atmospheric Chemistry and Physics Discussions

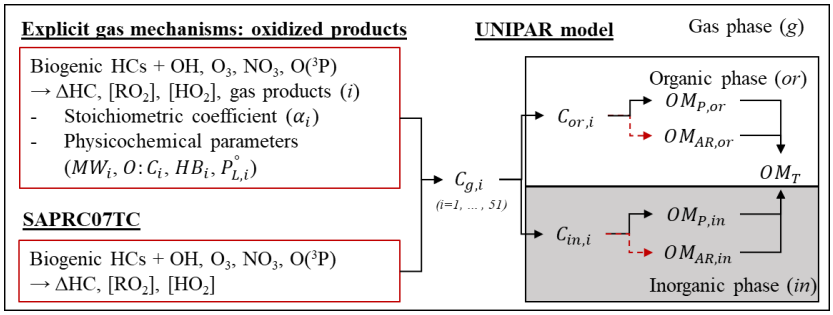

Figure 1. The model structure of the UNIPAR model coupled with SAPRC07TC gas mechanism with model parameters originated from the explicit gas mechanisms. The lumping species and their model parameters were estimated by simulating the explicit gas mechanism and applied to the UNIPAR model simulation. $C_{g,i}$, $C_{or,i}$, and $C_{in,i}$ are the concentration of organic compound (i) in gas phase (g), organic phase (or), and inorganic phase (in). $OM_{p,or}$ and $OM_{p,in}$ is the SOA mass generated via gas-particle partitioning in or and in, respectively. $OM_{AR,or}$ and $OM_{AR,in}$ is the SOA mass generated via in-particle chemistry in or and in, respectively.

https://doi.org/10.5194/acp-2022-327
Preprint. Discussion started: 24 May 2022

Atmospheric Chemistry and Physics Discussions

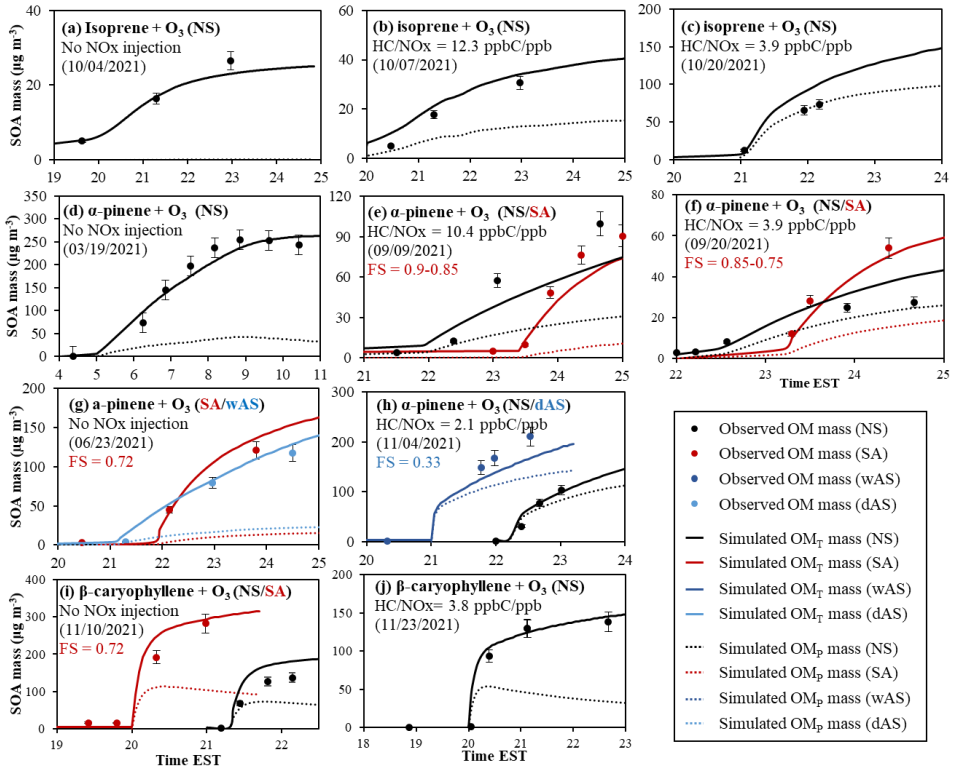

Figure 2. Observed (symbols) and simulated SOA mass (line) for the ozonolysis of isoprene ((a)-(c)), α-pinene ((d)–(h)), and β-caryophyllene ((i) and (j)) at different seed conditions and NO_x levels. SOA mass concentrations are corrected for the particle loss to the chamber wall. The simulated OM_T (solid line) and OM_{AR} (dotted line) are also illustrated. The error (10%) associated with SOA mass was estimated with the instrumental uncertainty.

https://doi.org/10.5194/acp-2022-327
Preprint. Discussion started: 24 May 2022

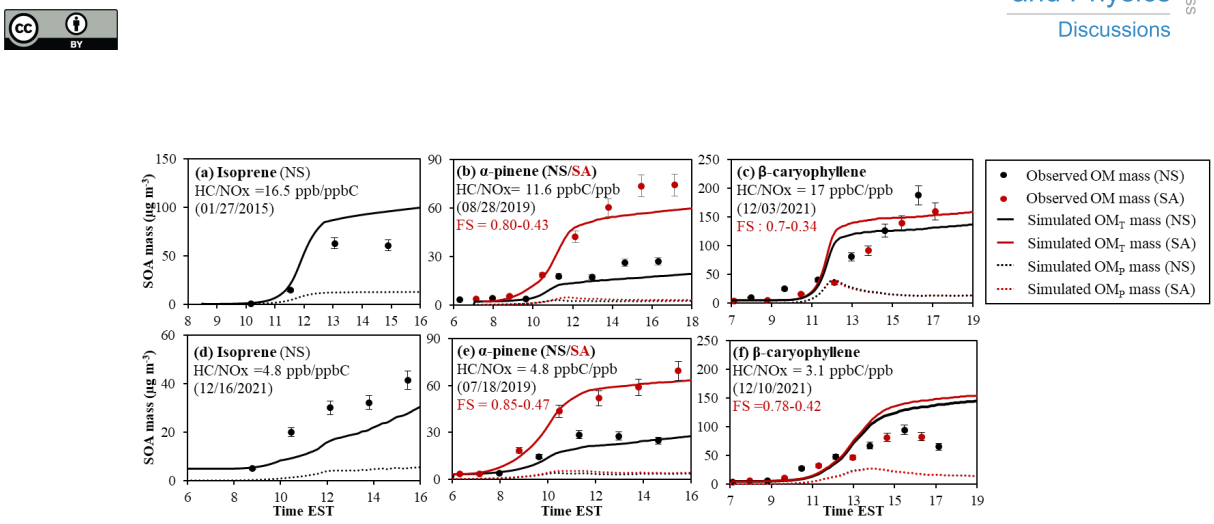

Figure 3. Observed (point) and simulated SOA mass (line) for the photooxidation of isoprene ((a) and (d)), α-pinene ((b) and (e)), and β-caryophyllene ((c) and (f)) at different seed conditions and NO_x levels. SOA mass concentrations are corrected for the particle loss to the chamber wall. The simulated OM_T (solid line) and OM_{AR} (dotted line) are also illustrated. The error (10%) associated with SOA mass was estimated with the instrumental uncertainty.

https://doi.org/10.5194/acp-2022-327
Preprint. Discussion started: 24 May 2022

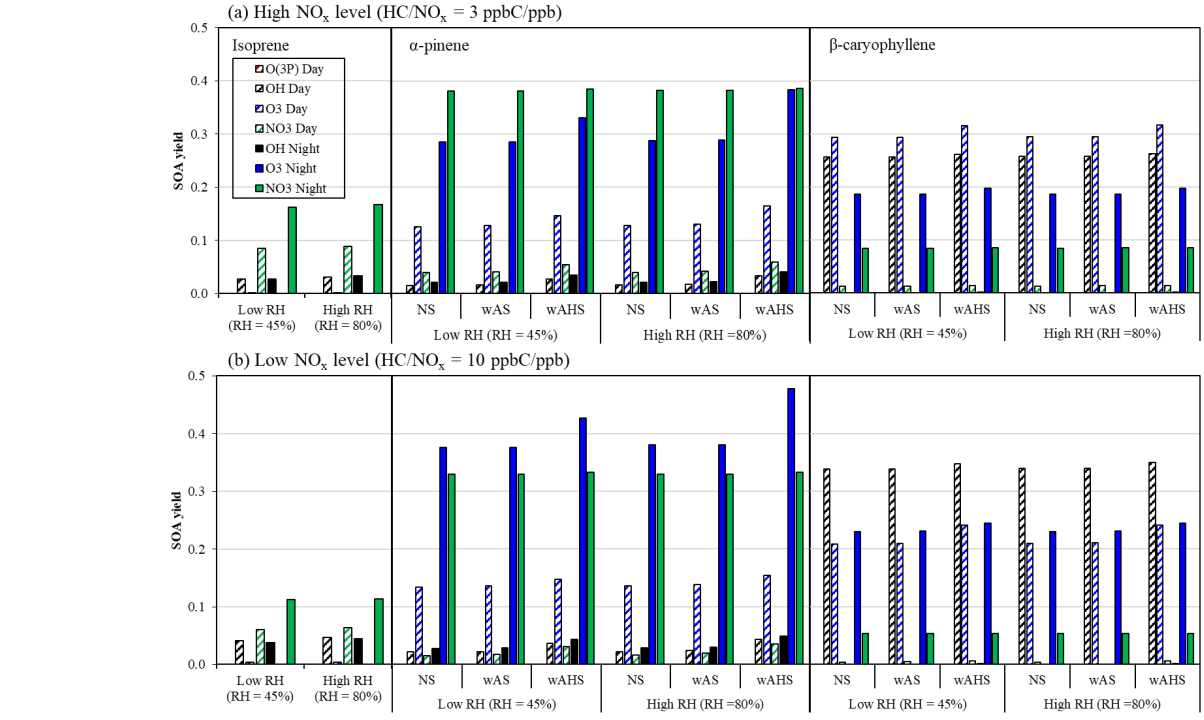

Figure 4. The potential SOA yield from each oxidation path from the given HC consumption under (a) high NO_x level (HC/NO_x = 3 ppbC/ppb) and (b) low NO_x level (HC/NO_x = 10 ppbC/ppb). The consumption of biogenic HC was set to 50 ppb (138 μg m^{-3}), 30 ppb (162 μg m^{-3}), and 20 ppb (167 μg m^{-3}) for isoprene, α-pinene, and β-caryophyllene, respectively. The SOA formation was simulated at 298K under two different RH (45% and 80%) with 10 μg m^{-3} of OM_0. For the α-pinene and β-caryophyllene, the SOA formed at three different seed conditions (NS, wAS, wAHS).

https://doi.org/10.5194/acp-2022-327
Preprint. Discussion started: 24 May 2022

Atmospheric Chemistry and Physics Discussions

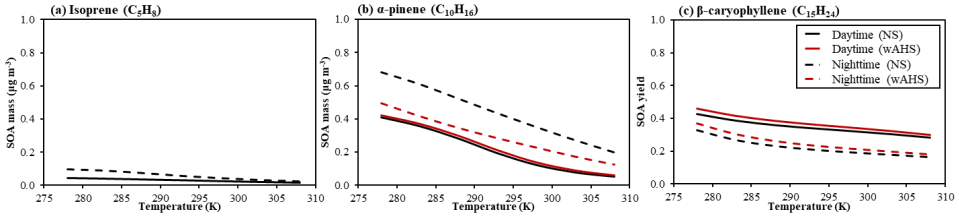

Figure 5. The biogenic SOA yield from (a) isoprene, (b) α-pinene, and (c) β-caryophyllene in both daytime (solid line) and nighttime (dashed line) under the various temperature, ranging from 278K to 308K. The HC/NO_x level was set to 3 ppbC/ppb. The SOA formation was simulated with 10 μg m^{-3} of OM_0 at the 50% of RH with the fixed initial concentration of isoprene, α-pinene, and β-caryophyllene at 50 ppb, 30 ppb, and 24 ppb, respectively. The daytime SOA formation was simulated under the reference sunlight intensity (Fig. S1), which was measured on 06/19/2015 at the UF-APHOR. The wall-free model parameters were applied to simulate SOA formation (Han and Jang, 2022).

https://doi.org/10.5194/acp-2022-327
Preprint. Discussion started: 24 May 2022

Atmospheric Chemistry and Physics Discussions

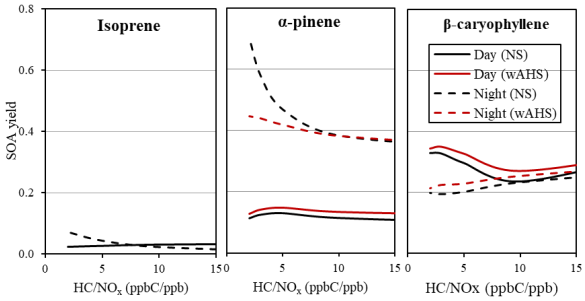

Figure 6. The biogenic SOA yield from (a) isoprene, (b) α-pinene, and (c) β-caryophyllene in both daytime (solid line) and nighttime (dashed line) under the various NO_x levels. The RH and temperature were set to 50% and 298 K, respectively. The SOA formation was simulated with 10 μg m^{-3} of OM_0 with the fixed initial concentration of isoprene, α-pinene, and β-caryophyllene as 50 ppb, 30 ppb, and 24 ppb, respectively. The daytime simulation is performed under the reference sunlight intensity (Fig. S1) which was measured on 06/19/2015 at the UF-APHOR. The wall-free model parameters were applied to simulate SOA formation (Han and Jang, 2022).

https://doi.org/10.5194/acp-2022-327
Preprint. Discussion started: 24 May 2022

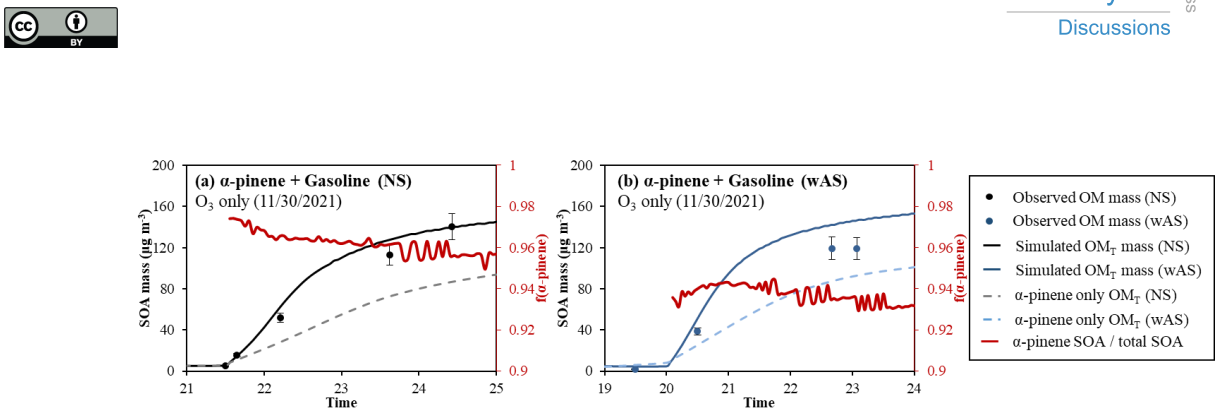

735 Figure 7. Observed (symbol) and simulated SOA mass (line) for the ozonolysis of α-pinene in the presence of gasoline fuel (a) without and (b) with wet-AS seed. SOA mass concentrations are corrected for the particle loss to the chamber wall. The simulated OM_T (solid line) in the presence of gasoline fuel and that in the absence of gasoline fuel (dashed line) are also illustrated. The dashed lines denote the simulated SOA mass in the absence of gasoline fuel under the same experimental conditions. The fraction of α-pinene SOA to total SOA (f(α-pinene)) are illustrated in red lines. The error (10%) associated
740 with SOA mass was estimated with the instrumental uncertainty.